TRR

Research Article

Actuated Traffic Signal Performance Evaluation along Arterials using Wi-Fi Travel Time Samples and High-Resolution Traffic Signal Events Data

Pengfei (Taylor) Li[1], Farzana R. Chowdhury[1], Peirong (Slade) Wang[1], and Sayem Mohammad Imtiaz[2]

Abstract
Understanding traffic progression on arterials is critical for traffic signal control and urban traffic management. Traffic conditions are highly dynamic and evolve over time. Therefore, it is necessary to evaluate the arterial's performance periodically to determine how well a traffic signal system is functioning. Arterial performance is conventionally evaluated based on travel time/speed collected via the probe vehicles. New approaches based on high-resolution traffic signal events have been proposed by a group at Purdue University, based on the Purdue Coordination Diagrams (PCDs). Both traditional arterial travel times/speeds and the PCDs can effectively reflect the level of traffic progression on arterials, while some practical questions have been raised about how to synthesize these two methods. The framework proposed in this paper integrates two types of performance measures by defining new multi-intersection coordination diagrams to examine traffic signal performance. The multi-intersection coordination diagram under different speeds can provide a straightforward tool for informed offset adjustments of actuated traffic signal coordination. In contrast, the state-of-the-practice traffic coordination performance analysis relies on fixed timings and empirical fine-tuning in the field. It is expected that these efforts can provide new insights to practitioners on how to use emerging traffic data better to improve the performance of actuated traffic signal operations on arterials.

Traffic signal performance and traffic progression on arterials is important for everyday traffic operations. Conventionally, traffic signal performance on arterials is evaluated based on end-to-end travel time or speed. According to the Highway Capacity Manual 2010 (*1*), the level of service (LOS) of an arterial is defined as the travel speed experienced as opposed to the posted speed limit.

In recent years, research efforts have been dedicated to the exploration of new measures of effectiveness (MOEs) for arterials as well as new approaches to data collection for this purpose. Among the numerous efforts, one of the exceptional achievements has been that of Dr Darcy Bullock's group at Purdue University which has designed and proved new traffic signal performance measures using high-resolution traffic signal events data. Another important research achievement by the same group is to estimate travel time or space travel speed via capturing and matching unique "signatures" of vehicles at different locations. These two achievements are

contributing to traffic signal performance across the country today. They are presented in more detail in the literature review, below.

Practitioners have expressed an interest in better synthesizing these two efforts. It has been seen that the availability of big data on traffic is substantially changing daily traffic signal practices, and triggering new research needs for exploring the additional potential of multi-source traffic data in traffic signal operations. In this paper, we present our research efforts in exploring new MOEs for actuated traffic signal performance through integrating multi-source traffic data. The traffic data we used include arterial travel time/space speed data

[1]Department of Civil Engineering, University of Texas Arlington, Arlington, TX
[2]Department of Computer Science, Iowa State University, Ames, IA

Corresponding Author:
Pengfei (Taylor) Li, Taylor.Li@uta.edu

samples and high-resolution traffic signal events data. The research findings in this paper are practice-ready.

Literature Review

The reviewed literature is divided into two categories: (i) traffic signal performance evaluation based on high-resolution traffic signal events and (ii) travel time or space-mean speed estimation based on captured vehicle "signatures."

Traffic Signal Performance Evaluation Based on High-Resolution Traffic Signal Events

Traffic signal data are usually in an aggregated form, such as traffic volumes or percentage of green signal in 15 min. Such aggregations consequently miss the random nature of the travel of individual vehicles. Actuated traffic signal control systems are also randomly driven by the random arrival of vehicles. To address this issue, the research community began to discuss the possibility of collecting individual traffic signal events generated during traffic signal operations. The need to exploring new MOEs and new evaluation methods for arterials was raised in the late 1990s. One of the earliest research efforts can be traced back to 2001, when Abbas et al. developed a real-time offset tuning algorithm according to individual vehicle arrivals (2, 3). Day et al. made a quantitative analysis of coordination for both fully actuated and fixed traffic control systems based on individual signal phase transitions (4). The selected MOEs include equivalent hourly volumes, green durations, volume over capacity (v/c) ratios, and Highway Capacity Manual arrival types. Later, Day et al. designed new diagrams based on traffic signal events to demonstrate the performance of traffic signal systems, now commonly referred to as Purdue Coordination Diagrams (PCDs) (5). One of the most popular MOEs is the number of arrivals on green at an intersection. The rationale is that if most vehicles arrive during the green, they will cross that intersection without delay, suggesting an effective coordination between the adjacent intersections. The percentage of green time is estimated based on the traffic phase transition events, and then offsets are optimized. The authors also use the Bluetooth probe travel time data to evaluate the impact of offset changes.

The invention of PCDs has been receiving wide attention in the community ever since, and the research group at Purdue University has proposed many applications to arterial traffic operations based on the traffic signal events. For example, Day et al. compared the effectiveness of multiple algorithms for offset optimizations such as the quasi-exhaustive search, Monte Carlo selection, genetic algorithms, hill climbing, and the combination method using the link-pivoting version for arterials (6). From the comprehensive analysis of the computational efficiency of the above algorithms, the authors concluded that the combination method was able to find the most optimal solution whereas the Monte Carlo selection and the quasi-exhaustive search did not give satisfactory results for the optimal solution. Day et al. also applied wireless magnetometer sensors to capture vehicle arrival events at the signalized intersection for both actuated and coordinated system (7). In that study, wireless magnetometer performance was evaluated for two left-turn pockets, and the analysis results cross-compared with the performance of inductive loop detectors in relation to false calls, missed calls, activation, and termination latency. The experiment began with placing one magnetometer in the center of each loop detector and was further modified by adding two more magnetometers in the left-turn lanes. The test results showed that both wireless detectors and inductive loop detectors gave identical outputs for false calls and missed calls.

In parallel to the above arterial traffic signal performance, note that high-resolution traffic signal events are also applied to the identification of oversaturated intersections based on traffic shockwave theories (8) and queue estimation at oversaturated intersections (9) by Henry Liu's then research group at the University of Minnesota.

Travel Time Estimation Based on Captured In-Vehicle Bluetooth/Wi-Fi MAC Addresses

According to the Highway Capacity Manual since 2010, the LOS on arterials is defined as actual space-mean travel speed as opposed to the posted speed limit (see Table 1). Since travel time is the inverse of space-mean travel speed, end-to-end arterial travel times are collected regularly by public agencies to evaluate the traffic signal performance. In traffic applications, Haseman et al. used automatically-collected Bluetooth probe data to estimate travel mobility metrics in work zones (10). The

Table 1. Arterial Level of Service (LOS) as Defined in *Highway Capacity Manual 2010*

Travel speed as a percentage of basic free-flow speed (%)	LOS by critical volume-to-capacity ratio	
	≤1.0	>1.0
>85	A	F
>67–85	B	F
>50–67	C	F
>40–50	D	F
>30–40	E	F
≤30	F	F

information collected through the Bluetooth devices is displayed on the traffic application website to offer motorists a better informed selection of route plans during their trips. This dataset is also applicable to estimation of crash probability since queuing often leads to an increase in crash rate. This real-time monitoring offers a mechanism for reliable travel time analysis. Brennan et al. used captured Bluetooth Media Access Control (MAC) addresses and applied the traditional algorithm of license plate study to approximate travel time and origin-destination matrix (*11*). They concluded that the efficiency of the Bluetooth MAC address collection is not related to the traffic volumes and is rather sensitive to the height of the antenna. Day et al. (*12*) conducted a performance analysis along an arterial considering the travel time reliability metrics according to the collected Bluetooth probe vehicle data. The raw data were collected every minute and then aggregated into 15-min intervals. Hainen et al. used collected Bluetooth MAC addresses to predict drivers' route choice and travel time reliability under unexpected road conditions (*13*). Martchouk et al. also used the Bluetooth technique to observe the possible reasons for travel time variation on freeways (*14*). Young et al. applied multiple vehicle identification techniques to visualize arterial performance (*15*). In their research, they re-identified vehicles to evaluate the corridor traffic performance. The data samples included: license plate matching, electronic tolling ID matching, and Bluetooth and Wi-Fi MAC addresses matching. The corridor performance is visualized by overlaying plots and cumulative frequency diagram to identify the trends of travel time changes along a corridor or road segment. Remias et al. compared several approaches to collecting probe vehicle data such as GPS, pavement sensors, capturing Bluetooth MAC addresses, crowd-sourced data, and virtual probe data (*16*). Through this comparison, it was shown that, although the Bluetooth MAC address matching cannot collect a high penetration of samples compared with reidentification pavement sensors, it is more cost-effective and portable.

A Wi-Fi device normally needs to exchange its MAC address with the Wi-Fi access point (AP) to identify the AP, further seek authentication and association, or both. In most personal portable devices, the Wi-Fi module is configured to transmit its MAC address into the air continuously to search for nearby APs. Note that such a process is an unencrypted broadcast and a third-party Wi-Fi sniffer can discover those transmitted data packets containing individual Wi-Fi MAC addresses. Because of the fundamental difference between Bluetooth and Wi-Fi technologies, capturing the Wi-Fi MAC addresses reveals advantages over the Bluetooth solution in estimating travel times. For instance, Wi-Fi sensors can capture as many of the available MAC addresses as possible

at little latency, whereas the Bluetooth sensors can at most randomly capture seven MAC addresses at up to 10 s latency.

Methodology

This section includes the methods to generate new arterial traffic signal performance measures based on the high-resolution traffic signal events and travel time estimation based on captured in-vehicle Wi-Fi MAC addresses.

Multi-Intersection Coordination Diagram for Actuated Traffic Signal Control Systems

A new multi-intersection coordination diagram is designed based on high-resolution traffic signal events. Based on the multi-intersection coordination diagram, new MOEs for arterial traffic signal performance are designed.

Effective Green Bandwidth and Band Attainability in Actuated Traffic Coordination. The concept of "green band" is fundamental to time-based traffic (signal) control coordination. Most traffic control coordination aims to maximize the green bandwidth so that vehicles within the band can cross multiple intersections without stops. In practice, the bandwidth is maximized by adjusting local timing plans, common cycles, and offsets at intersections. This band-based traffic control coordination has proved to be effective in many cases. Nonetheless, for actuated traffic control coordination, the effective bandwidth is different from the theoretical calculation. According to the mechanism of actuated traffic control, if a side-street phase gaps out and a floating force-off is set, then any unused green on side streets will be returned to the coordination phase to favor the mainline traffic. This mechanism is referred to as "early return to green." As shown in Figure 1, when the coordination phase starts early, vehicles will also be released early. As a result, when they reach the next intersection, the downstream green has not yet started and so all vehicles must stop and this can create delays. On the other hand, if the mainline greens at both intersections start early, the effective bandwidth is larger than the programmed values. Calculating green bandwidths according to programmed traffic coordination plans for actuated traffic control coordination could be misleading.

To address this issue, we propose a new concept, namely "effective green bandwidth" for actuated traffic control coordination. The effective green bandwidth within a time period is defined as the total established green bandwidth within a time period. Figure 2*a* demonstrates how to calculate the effective green bandwidth.
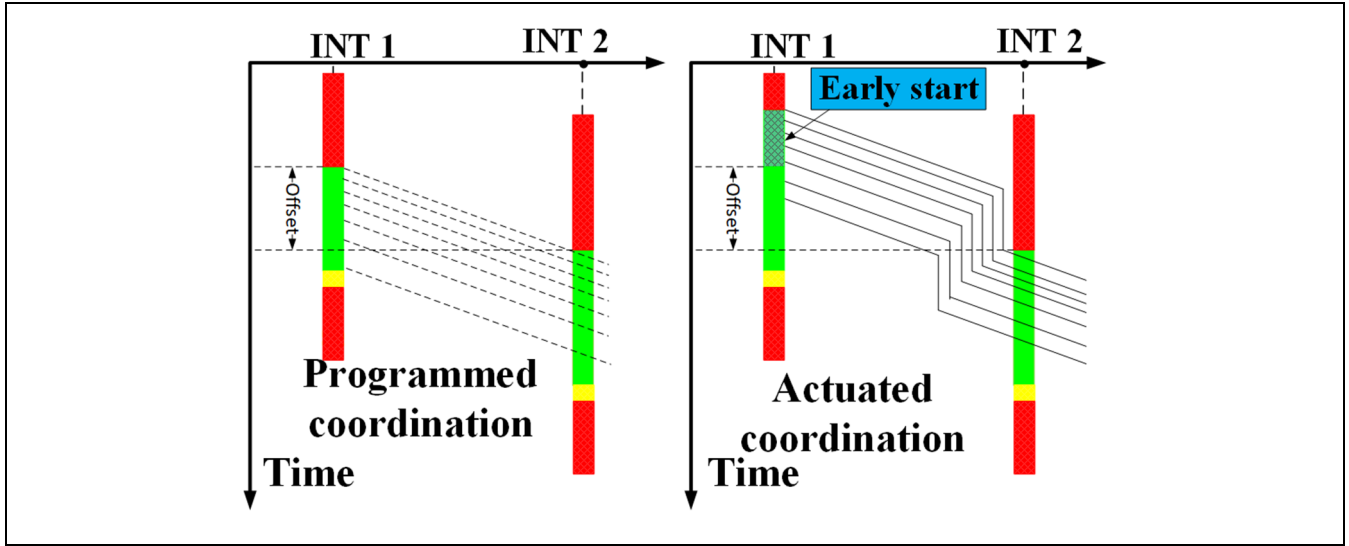
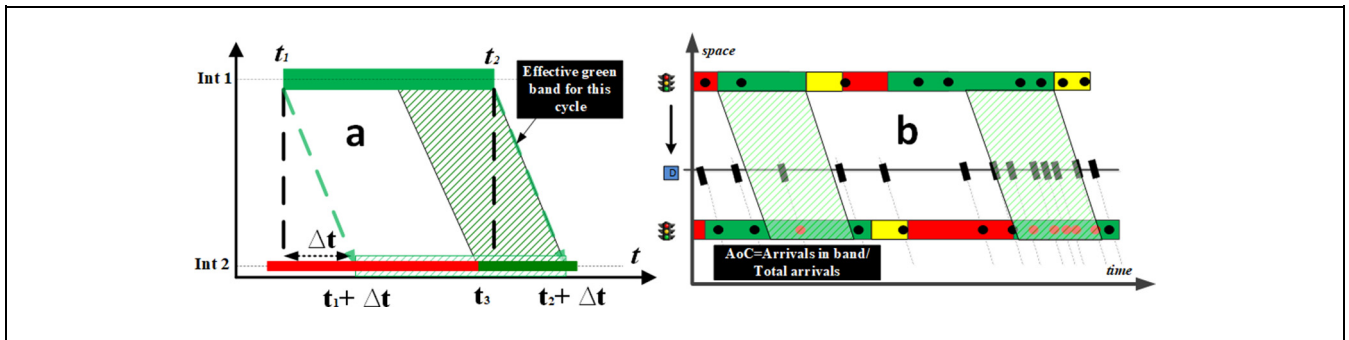**Figure 1.** Illustration of "early return to green" in actuated traffic coordination.

Figure 2. Calculation of effective green bandwidth, arrivals on coordination, and band attainability for actuated traffic signal control systems.

With a cycle, assume the mainline green starts at t_1 and ends at t_2 and vehicles take Δt to reach the next intersections; then we can set a band time window at the downstream intersection from $t_1 + \Delta t$ to $t_2 + \Delta t$. Within that time window, a green band can be established only after t_3 and the effective bandwidth is $(t_2 + \Delta t - t_3)$. The ratio of total established green band length divided by the total green durations at downstream intersections with a period is referred to as band attainability. The band attainability indicates how much mainline greens are actually used for traffic control coordination. A similar theoretical concept was also proposed by Tian et al. (17). Note that Figure 2a only illustrate one scenario of establishing an effective green band, there are also other scenarios of establishing green bands. For instance, if the downstream green in Figure 2 ends at t_4 which is earlier than $t_2 + \Delta t$, then the effective band will be $(t_4 - t_3)$.

Calculation of band attainability can be formulated as:

$$BA = \frac{\sum EGB_i}{G} \qquad (1)$$

where BA : is band attainability; EGB_i is the effective green band in the ith cycle; and G is total green time.

While establishing the effective green band, we ignore the effects of traffic dispersion while vehicles are discharged to downstream intersections. Day and Bullock applied Robertson's traffic dispersion model (18) and downstream detector events to estimate the source of arrivals as well as to calibrate the traffic dispersion model (19). Hainen et al. in their studies of diamond interchanges also distinguished the sources of arrivals according to the time when upstream greens start (20).

Arrivals on Coordination. Standard PCDs focus on individual intersections and adopt the percentage of arrivals on green to represent the level of traffic progression. Its rationale is that vehicles will mostly arrive on green along

arterials only if the traffic coordination plan is effective. Based on the same rationale, we propose a new multi-intersection coordination diagram. With the same type of traffic signal event data, another form of PCDs is proposed.

As shown in Figure 2*b*, the actual traffic control plan is first plotted according to the phase transition events at each studied intersection. Then individual vehicle arrivals are plotted on top of the traffic timing plans over time (see the dots in Figure 2*b*). At each intersection, Figure 2*b* contains the equivalent information as the standard PCDs and the arrivals on green is the total number of dots falling into the greens.

Arrivals on green (AoG) is defined as the ratio of the vehicle arrivals during green as opposed to the total arrivals within the study period. Arrivals on coordination (AoC) is an extension of AoG because AoC further distinguishes arrivals on green into two types: (i) arrivals on green from the upstream coordinated intersection and (ii) arrivals on green from the upstream side streets or intermediate drive ways. In Figure 2*b*, the number of dots in greens divided by the total dots is AoG while all the red dots divided by the total arrivals in greens is AoC.

AoC can be calculated as follows:

$$AOC = \frac{n_g}{N} \tag{2}$$

where n_g is number of vehicles arriving within the established green bands from the upstream intersection to the current (downstream) intersection; N is the total number of vehicle arrivals in the study period

Effective Volume/Capacity Ratios on Mainline Streets for Actuated Traffic Control. The volume/capacity (v/c) ratio is a popular indicator of traffic congestions at intersections. According to the Highway Capacity Manual (*1*), the v/c ratio on one approach for a fixed timing plan is calculated as follows.

$$\left(\frac{v}{c}\right)_i = \frac{v_i}{s \times \frac{g_i}{C}} \tag{3}$$

where v_i is the traffic volume on approach i; s is the the saturation rate; g_i is the effective green duration on approach i; and C is the cycle length.

In an actuated traffic control system, g_i and C may change from cycle to cycle. Therefore, using the programmed g_i and C to calculate the v/c ratio of actuated traffic control systems might bring bias to the v/c calculation. Based on the high-resolution traffic signal events data, it is possible to capture all the arrivals on one mainline approach and calculate the total green times during a time period. As such, the effective v/c within a time period can be accurately calculated. If the effective v/c

ratio is greater than 1 within a period, it implies that cycle failures have likely occurred.

The modified actuated v/c ratio is:

$$\left(\frac{v}{c}\right)_i = \frac{v_i}{s \times \frac{\sum_{m=1}^{n} g_{i,m}}{T}} = \frac{v_i}{s \times GT} \tag{4}$$

where T is the duration of the study periods; s is saturation rate; v_i is total vehicle arrivals on approach i during T; $g_{i,m}$ is effective green on approach i in m^{th} cycle; and GT is green time percentage.

Using phase transition events and Equation 3, we can identify each cycle failure; Equation 4 provides an alternative method to identify consistent cycle failures within a period. Even under effective timings, temporary cycle failures are inevitable given the random nature of arrivals. Temporary cycle failures should be acceptable in practice if the residue queue is cleared soon. In this study, we focus on capturing consistent cycle failures, identified through comparing hourly capacity and hourly arrivals.

Arterial Travel Time Estimation with Wi-Fi MAC Addresses and the Kalman Filter Method

The Wi-Fi travel time estimation is via a prototype Wi-Fi MAC address collecting device built by the authors. It turns out that the matched travel time samples contain many outliers and much noise. To offer a valid travel time estimation, effective processing algorithms are necessary to filter the outliers and estimate the travel times. We have developed a travel time estimation algorithm based on the Kalman filter framework.

Once a raw Wi-Fi travel time sample is generated, empirical thresholds are first applied to filter obvious outliers. A travel time sample is considered valid only when it is between 50% of free-flow travel time and 300% free-flow travel time. Please note that the 300% free-flow arterial travel time is arbitrary and so it is subject to changes in very congested areas. According to the central limit theorem in statistics, we can safely assume the travel time samples (t_i) are normally distributed and the unbiased travel estimator $\hat{\mu}$ and the variance $\hat{\sigma}^2$ can be estimated as in Equation 5:

$$\hat{\mu} = \sum_{i=1}^{m} t_i, \hat{\sigma}^2 = \frac{\sum_{i=1}^{m} (t_i - \hat{\mu})^2}{m} \tag{5}$$

In practice, it is common to see that the number of samples within a time period may be low or even zero. In that case, inherent randomness of travel time samples will govern the travel time estimation and generate large fluctuations. To mitigate this issue, we use a weighted average of two consecutive periods (current period k and immediately past $k - 1$ period) to smooth the travel time estimations. This operation will help to enhance the

algorithm's tolerance to variations. It is formulated as in Equation 6.

$$\hat{\mu}_k = \left(\frac{m_k}{\max\left(0.01, m_k + \max\left(0, \left(1 - \frac{\Delta t}{T}\right)\right)m_{k-1}\right)} \right)\hat{\mu}_k$$
$$+ \left(1 - \frac{m_k}{\max\left(0.01, m_k + \max\left(0, \left(1 - \frac{\Delta t}{T}\right)\right)m_{k-1}\right)} \right)\hat{\mu}_{k-1}$$

$$(6)$$

where Δt is the sampling period (e.g., 900 s) and T is the maximal time interval beyond which even two consecutive sampling periods are considered independent (e.g., 3,600 s).

Equation 6 suggests that the correlation between two consecutive sampling periods decreases with the increase of sampling periods because the weight value $\left(1 - \frac{\Delta t}{T}\right)$ of previous samples decreases. When the time interval reaches T or longer, two consecutive sampling periods are considered independent. The weights of former valid samples are also linearly discounted with the increase of time intervals. Under an extreme situation, if the sample size is zero in one period ($m_k = 0$), then the estimated travel time during period k–1 is used as its approximation ($\hat{\mu}_k = \hat{\mu}_{k-1}$).

Based on the relevant literature on the measuring errors, we propose a Kalman filter algorithm to estimate the travel times. The Kalman filter framework is widely used to estimate the true state of a linear dynamic system by minimizing the mean squared error. Although the traffic systems on arterials are nonlinear by nature, various successful linearization efforts have been reported in the past, such as the first-order traffic flow model because of Newell (*21, 22*). With the Kalman filter framework, the system measuring errors are explicitly modeled (*23*). It is an efficient Bayesian estimating process except that the state space of the latent variables and observed variables are continuous and must be consistent with the normal distributions. A Kalman filter contains two steps: *Predict* and *Update*. The predicting step is to make an initial estimation of the system's current state. In this paper, the system state is estimated travel time during a sampling period. Before an estimation starts, the initial state is assumed to be the same as the immediately past travel time and then updated with the new travel time samples within the current period. Mathematically, the Kalman filter approach can be formulated as follows. All the matrices and variables are of one dimension.

$$t_k = F_k t_{k-1} + B_k u_k + w_k \qquad (7)$$

During the period k, an observation (travel time sample) z_k is generated with:

$$z_k = H_k t_k + e_k \qquad (8)$$

where

- t_k = the travel time during the period k;
- F_k = Kalman state transition matrix during period k. In our case $F_k = 1$;
- B_k = the control-input model of control vector u_k during period k;
- H_k = the observation matrix in the Kalman filtering during period k;
- e_k = the measuring error ($e_k \sim \phi(0, R_k)$) during period k;
- w_k = the system white noise ($w_k \sim F(0, Q_k)$) during period k.

It should be noted that when travel time is collected on arterials, the real travel time is affected not only by traffic volumes but also by the traffic control plans at intersections. Therefore, it is imperfect to assume the linearity of arterial systems. Nonetheless, we empirically modify and calibrate the Kalman filter model to fit into this context.

According to the literature (*24*), 97.5th percentile and 2.5th percentile travel speeds are 14.7 ft/s (10 mph) above and below the average speed. The 95% confidence interval ($t_{2.5\%}, t_{97.5\%}$) can be calculated as $t_{2.5\%} = \frac{L}{\bar{u} + 10 \times 1.47}$ and $t_{97.5\%} = \frac{L}{\bar{u} - 10 \times 1.47}$ (in feet and seconds). Q_k in w_k (the system noise) in Equation 7 is then calculated as:

$$\sigma_t = \frac{(t_{97.5\%} - t_{2.5\%})}{2 \times z_{0.025}} \qquad (9)$$

where $z_{0.025}$ is the normal Z value 1.96.

R_k (or e_k) in Equation 8 is determined by the Wi-Fi sensor's measurement errors discussed above and $H_k = 1$ because the travel time is directly measured. After all the parameters are determined, travel time estimation can be described as in Algorithm 1:

Lastly, Equation 6 is applied to get the final travel time estimation for this period.

Note that Equation 9 does not effectively consider the control delays on arterials and there are no widely accepted travel time distributions on arterials. Therefore, the thresholds may have to be empirically adjusted in practice.

Case Studies: Arterial Traffic Signal Performance Evaluation in Starkville, Mississippi

In this section, we present the novel presentations of arterial traffic signal performance along Highway 12 in Starkville, MS.

Algorithm 1: Travel time estimation algorithms based on the Kalman filter framework

---

Assume m_k valid travel time samples, z_k^i ($i=1, 2\ldots, m_k$) are collected during period k. Link length and free-flow travel time are both known.

    Step 0: Initialization: when $k = 0$ (e.g., midnight), $t_0 = \frac{L}{u_f}$, w_k's variance $Q_{k=0}$ is calculated with Equation 9;

    Step 1: For each period k ($k=1, 2 \ldots$)

           Predict the travel time with Equations 5 and 6 as the a priori estimation

           Estimate variance: $P_k^- = P_{k-1} + Q_k$

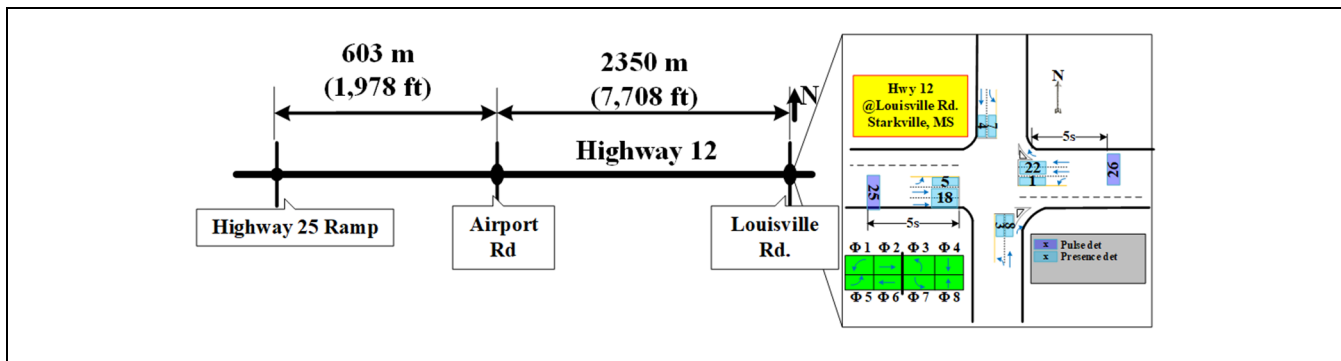   Step 2: Calculate the Kalman gain: $K_k = P_k^- (P_k^- - R_k)^{-1}$ (R_k is the variance of measure errors)

    Step 3: Update the posteriori state estimate: $\hat{t}_k = \hat{t}_k^- + K_k(z_k^i - \hat{t}_k^-)$

           Covariance update: $P_k = (I - K_k)P_k^-$

    Step 4: If $i < m_k$, then $i = i + 1$ go to step 3; otherwise i = 0, k = k + 1 and go to Step 2

    Step 5: If $i < m_k$, algorithm stops and the final travel time is retrieved as the estimate travel time during period k

---

Figure 3. Layout of the studied arterial.

PCDs with Arterial LOS at Individual Intersections

Three units of Wi-Fi MAC capturing devices were deployed at three intersections along Highway 12 in Starkville, MS. The intersections are controlled by Siemens Linux M60 controllers and the speed limit is 45 mph. The distances between intersections are shown in Figure 3.

At each intersection, additional detector zones are added into the Wavetronix sensors. Figure 3 shows the detector configuration at one of the intersections at Louisville Road. The advance detectors were set 5 s away from the stop line.

Two types of data sets are used to generate the enhanced PCDs: (i) high-resolution traffic signal events; (ii) time-of-day arterial space travel speed estimated with Wi-Fi travel time samples.

Time-of-Day AoG and Arterial LOS. Figure 4a shows the enhanced PCDs with arterial LOS at one intersection for 24 h. The blue line is the hour-by-hour arterial speeds calculated with Wi-Fi sensors. The letters are the LOS measured hourly. From Figure 4a, we can see there are three coordination plans during a weekday: morning (from 7:00 a.m. to 8:30 a.m.), noon (from 11:00 a.m. to

1:30 p.m.), and evening (from 4:00 p.m. to 6:30 p.m.). The rest of the time is local free. It can also be seen that the longest delays were generated in the early afternoon when the arterial LOS dropped to level D. There are not many vehicles after midnight and so the mainline green continued for multiple cycles. Since the data were collected in summer, the side-street travel demand was still low even after 7:00 a.m. and so the "early return to green" occurred between 7:00 a.m. and 7:15 p.m. The 24 h are also divided into several periods according to the time-of-day plan. As shown in Figure 4a, the 24 h on that day were divided into seven periods. In each period, the corresponding AoG and effective green ratios are calculated respectively according to the high-resolution traffic signal events. The AoG was overall lower than 50% in the summer because the traffic signal coordination plans were developed primarily for the higher travel demands of school days.

Time-of-Day Effective V/C Ratios. The traffic signal systems at all three intersections are all actuated and so the effective v/c ratios should be used following Equation 4. The saturation rate was empirically set to 1,500 vehicles per hour per lane according to the field observations.
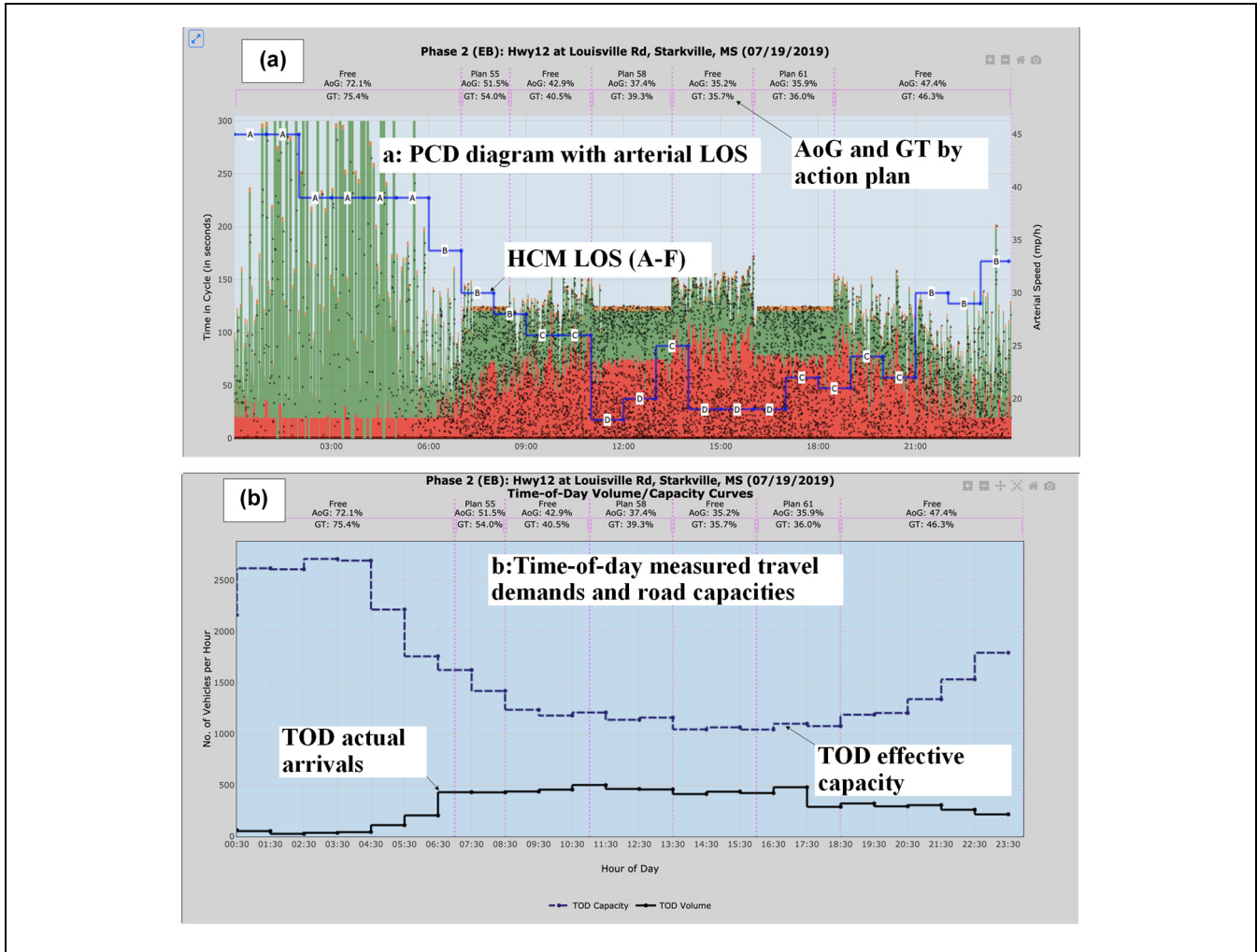
Figure 4. (a) Traffic Signal Performance of PCD and LOS; (b) TOD comparison of capacity and demand.
Note: AoG = arrivals on green; GT = green time percent; LOS = level of service; PCD = purdue coordination diagram; TOD = time of day.

Figure 4*b* shows the hourly travel flow rate (i.e., vehicle arrivals) and the effective road capacities according to the total green durations in that period. Figure 4*b* reveals that the provided road capacity (primarily for school days) is higher than the actual travel demand in the summer and so congestion is unlikely occur.

Figure 4*a* clearly reveals the consistency of two types of arterial traffic signal MOEs. From midnight to 7:00 a.m. is "local free" and traffic on side streets was very low. As a result, AoG and green percent were over 70% and the arterial LOS was A. With the increase of side-street traffic, the AoG and green percent gradually decreased and so did travel speed on the arterial. Between 1:00 p.m. and 4:00 p.m., the AoG and green time percent reached the lowest value and arterial travel speed also reached the lowest LOS (D). After that, both AoG and green time percent increased and the arterial travel speed also increased, suggesting better traffic progression.

The volume versus capacity diagram (Figure 4*b*) offers a new metrics to identify congestion. Ideally, the capacity curve (supply) should always be higher than the arrival curve (demand) to avoid congestion. If traffic is consistently congested, then the hourly v/c ratio will be greater than 1. As a result, the arrival curve will be higher than the capacity curve indicating the congestion. Another situation to identify congestion is that, if the queue length consistently increases and even reaches the advance detectors, then new arrivals cannot be detected, and we will see a sudden drop in the time-of-day vehicle arrival curve. It also implies possible over congestion.

Arterial Traffic Signal Performance with Multi-Intersection Coordination Diagram

An arterial traffic simulation model along Highway 12 was developed in VISSIM for additional experiments.
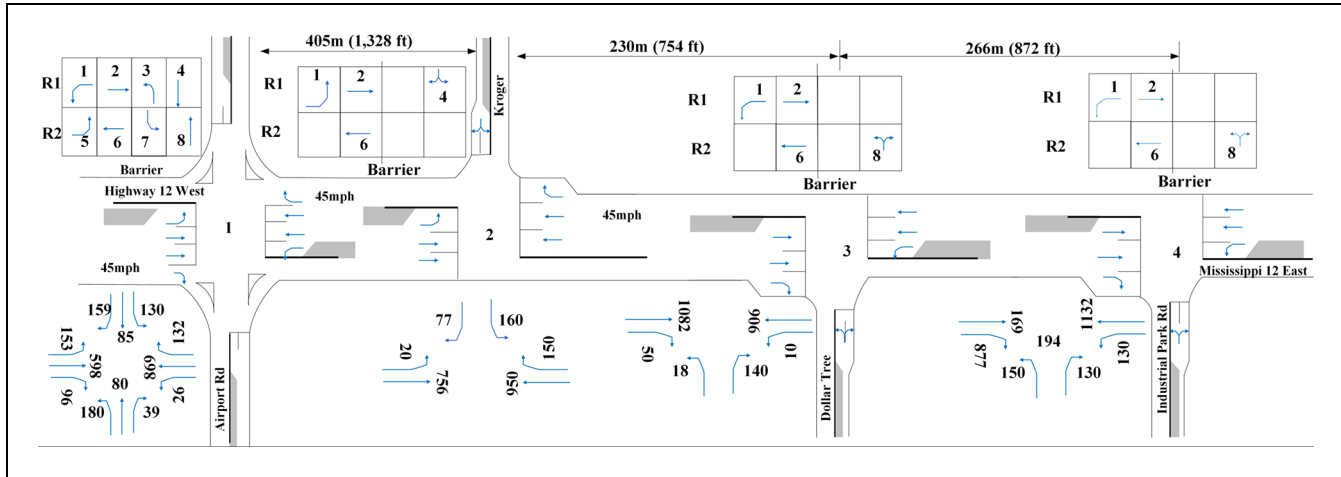
Figure 5. Layout of studied intersections.

The traffic signal simulation was established with the traffic signal software-in-the-loop emulators. The traffic signal emulator in PTV VISSIM, ASC/3, can output high-resolution traffic signal events and therefore the simulation environment almost has the same fidelity as in the field. It allows for more comprehensive evaluations under various scenarios. The traffic signal event data are generated using software-in-the-loop ASC/3 emulator via NTCIP protocols and so the data quality is comparable with the real-world traffic signal event logs.

Figure 5 shows the layouts of four intersections along Highway 12, the latest peak-hour turning movement counts, and the traffic signal phasing sequence. Compared with the road capacity, traffic is light and moderate. The detectors at each intersection are configured similarly with Figure 3. For each intersection, a local optimal traffic timing plan and a traffic coordination plan are developed using PTV Vistro.

Each simulation run lasts an hour during which four ASC/3 emulators generate traffic signal events, including the vehicle arrival detections and phase transitions

Effective AoG, AoC, GT, and BA under Local Optimal Traffic Signal Control Plans. We first calculate the values of AoG, AoC, and BA for a whole hour using the emulated traffic signal events data. The local timing plan is fully actuated and Figure 6a shows the varying effective greens for a few cycles. We can see that effective green bands can still be established even though all intersections are running local free. The multi-intersection MOEs are calculated only at downstream intersections, as shown in Figure 6a.

For westbound traffic, INT2 and INT3 have fairly large green time percentages (over 45.6%) because the travel demands on the side streets are very low. As a result, effective green bands between Intersections 4, 3, and 2 can be easily established and vehicle arrivals also

have good opportunities to cross those three intersections with stops. However, INT1's mainline green time percentage is reduced because of the high demand on other approaches. The AoG and AoC ratios between INT2 and INT1 are also low because the two intersections are not coordinated.

The pattern of eastbound traffic is similar; AoG and AoC ratios between INT1 and INT2 and between INT3 and INT4 are low because of the high volumes on the side streets at INT1 and INT4.

Effective Green, AoG, AoC, GT, and BA under Fixed Traffic Coordination Control Plans. We then evaluate the performance of a fixed traffic signal coordination plan with the newly proposed MOEs. The common cycle length for the four intersections is 110 s and the offsets from INT1 to INT4 are fine-tuned to 65, 39, 50, and 65 s, respectively. Comparing Figure 6a with Figure 6b, it is clear that the level of mainline traffic progression is better under fixed traffic signal coordination control than under local free timing plans. The AoG and AoC significantly increase. It is also noticed that the effective green time percentages increase as well because the mainline phases are not allowed to gap out.

Effective Green, AoG, AoC, GT, and BA under Actuated Traffic Signal Coordination Plans. In this experiment, we focus on a more common traffic signal configuration—actuated traffic signal coordination. The minor approaches can gap out to return the unused green back to the mainline.

Comparing Figure 6, *b* and *c*, we can see that the green time percentages increase at all intersections because of the early returns to the mainline green. Nonetheless, it is also noticeable that longer mainline greens do not necessarily help traffic progression because early release of
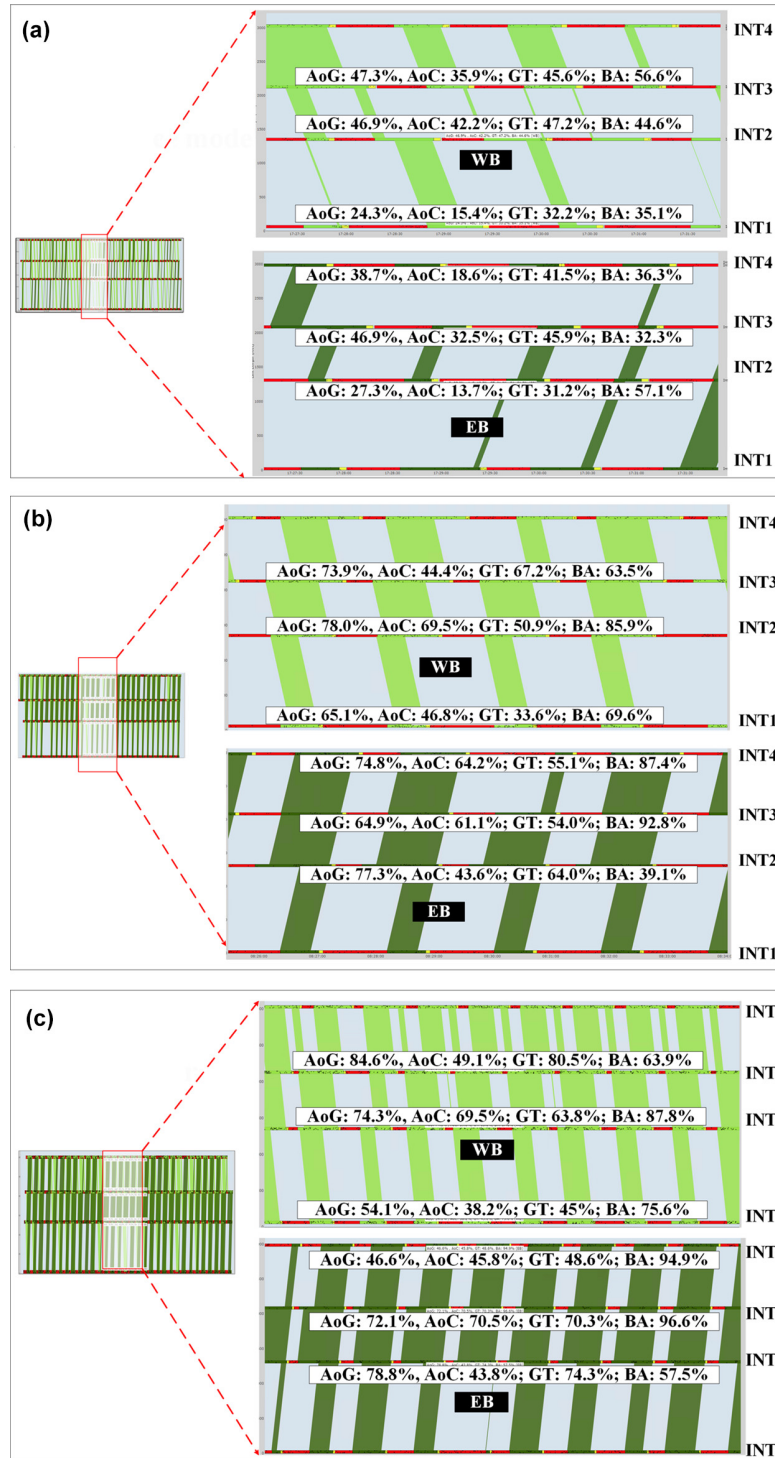
Figure 6. Multi-intersection measures of effectiveness under various traffic control strategies: (*a*) local free mode, (*b*) fixed coordination, (*c*) actuated coordination.
Note: AoC = arrivals on coordination; AoG = arrivals on green; BA = band attainability; GT = green time percent.

queues is detrimental to the establishment of green bands. For instance, the level of traffic control coordination turns out to decrease between INT1 and INT2 because

the arrivals within the established green band are fewer than those under the fixed traffic coordination timing plans. Therefore, we recommend that the actuated traffic
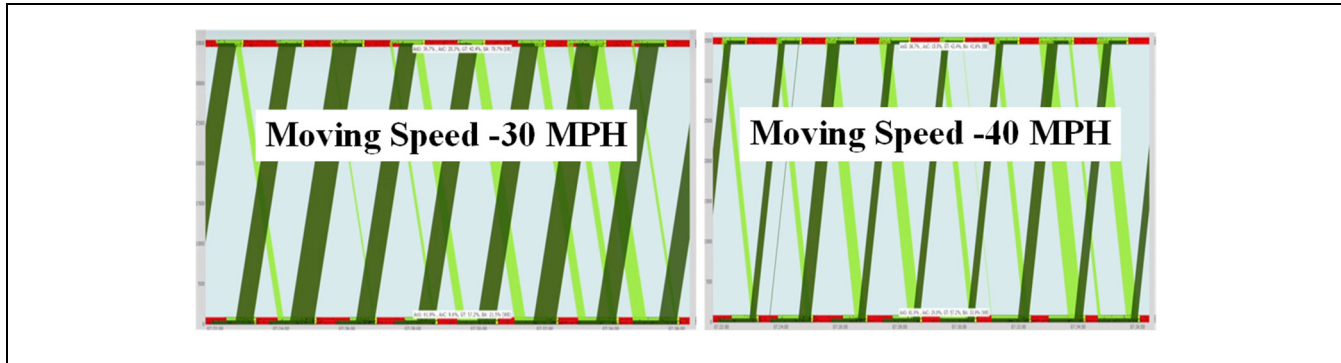
Figure 7. Effective green band at different moving speeds (same local phase transitions).

signal coordination strategy should be carefully selected because it may not be as helpful as the fixed traffic signal coordination strategy to the mainline traffic progression.

Figure 6 also shows the consistency of AoG and AoC values. They are close under all three control strategies in this experiment. The reason is that all four intersections are of major-minor type and therefore the mainline AoGs are mostly from the through traffic released at the upstream intersections. As such, AoC and AoG are almost the same. Nonetheless, it is expected that AoG and AoC will become significantly different if the upstream intersection is major-major and generates several platoons within a cycle.

Impact of Vehicle Moving Speed on Effective Green Bandwidth Calculation. AoG and green time percentage are not affected by the moving speed but the new AoC and BA are based on two consecutive intersections and thus are sensitive to the prevailing moving speed. A biased moving speed may change the results of AoC and BA. An alternative to using one value of speed for this purpose, designed by Hainen et al. (20), might be to use a slightly higher speed for the start of green and a slightly lower speed for the end of green.

In practice, the posted speed limit is often used to derive the time-space diagram and calculate the green bandwidth. If the moving speed is biased, the results may become misleading. To examine this speculation, we conduct an experiment to calculate the AoC and BA values using different moving speeds.

The calculation in Figure 6 is based on the posted speed limit of 35 mph. Let us assume two hypothetical scenarios: (i) drivers drive faster than the speed limit, such as 40 mph; (ii) drivers drive more slowly, because of congestion, at 30 mph. In both scenarios, the AoC and BA results turn out to be significantly different. Figure 7 shows differences of effective green bands because of different moving speed even though the local phase transitions are the same.

As an example, for the westbound traffic under fixed traffic signal coordination, if we change the moving speed from 35 mph to 30 mph, the AoC values change as:

- INT 3: 41.2% (3.2% decrease)
- INT 2: 53.4% (16.1% decrease)
- INT 1: 24.6% (22.2% decrease)

and the BA values change as:

- INT 3: 62.5% (23.4% decrease)
- INT 2: 76.7% (8.7% decrease)
- INT 1: 48.1% (21.5% decrease)

If we take a faster 40 mph as the moving speed, then the AoC values change as:

- INT 3: 42.0% (2.4% decrease)
- INT 2: 66.8% (2.3% decrease)
- INT 1: 44.0% (2.3% decrease)

and the BA values change as:

- INT 3: 62.3% (1.2% decrease)
- INT 2: 84.4% (1.5% decrease)
- INT 1: 64.8% (4.8% decrease)

From these results, we can conclude that the effective green bandwidth calculation (an indicator of traffic progression) is highly sensitive to the prevailing moving speed, especially when the moving speed is slower than the speed limit. The multi-intersection coordination diagram will provide a straightforward tool to evaluate the traffic progression along arterials under different moving speeds. The methods presented in this paper permit some informed adjustments or even optimization of those offsets to better accommodate arterial traffic signal operations where early return may occur.

In addition, it is also clear that the effective green bandwidth of actuated traffic signal systems is random

and varies cycle by cycle. Over time, we can get a distribution of the green bandwidth. Stochastic optimization for offsets shall be conducted to maximize the green bandwidth with the maximum likelihood. A similar concept was proposed by Yin et al. (*25*)

Conclusion and Future Work

In this paper, we present new performance measures for traffic signals on arterials based one multiple traffic data. The considered data include travel time samples via Wi-Fi probe vehicles and high-resolution traffic signal events. The standard PCD is first enhanced by synchronizing time-dependent travel speed and LOS on the arterial. This effort is to meet a rising need for integrating traditional arterial performance measures (arterial travel time/speed) with the emerging PCDs based on high-resolution traffic signal events. Based on the high-resolution traffic signal events data, we propose three new multi-intersection MOEs to evaluate actuated traffic signal system performance: (i) AoC to identify the number of vehicle arrivals during the established green bands. AoC can further distinguish arrivals from the upstream mainline during green from arrivals from the side streets during green; (ii) BA to identify how much mainline greens are used for traffic signal coordination; and (iii) effective v/c ratio to identify the possible cycle failures by comparing the travel demand and the effective road capacities under actuated traffic control systems.

The proposed multi-intersection coordination diagram reveals the sensitivity of green bandwidth calculation (i.e., traffic progression) to vehicles' prevailing moving speed between intersections. The state-of-the-practice approach is to use the posted speed limit to calculate the green bandwidth. The multi-intersection coordination diagram shows that even a small change in the vehicle moving speed can cause significant changes to effective green bandwidth. The multi-intersection coordination diagram can provide a straightforward tool to examine the traffic progression, in relation to effective green bandwidth, at different speeds.

It is also recommended that caution should be taken while implementing actuated traffic signal coordination strategy along arterials. As we observed in the experiment, the level of mainline traffic progression may even reduce compared with the fixed traffic signal coordination strategy because the early returns to mainline green break the programmed green bands.

In the future, we plan to explore new database engines for traffic signal events data management. It is estimated that daily traffic signal event logs at a standard intersection can range from 300,000 to 60,000 records. Data sets of such size should be ideally tackled by more powerful database engines instead of the traditional SQL database engine. In this study, we adopted the MySQL database engine to store and process data. To ensure computing efficiency, it was necessary to limit data storage up to 30 days and the diagram rendering for up to 24 h. In the future, we plan to explore other database techniques, like GPU database techniques, to further investigate the potentials of traffic signal events data.

Author Contributions

The authors confirm contribution to the paper as follows: study conception and algorithm design: Pengfei (Taylor) Li; literature review: Farzana Chowdhury and Pengfei (Taylor) Li; web interface programming: Sayem M. Imtiaz and Peirong (Slade) Wang; database design and development: Pengfei (Taylor) Li; conceptual illustration: Farzana Chowdhury and Pengfei (Taylor) Li; data collection: Peirong (Slade) Wang and Pengfei (Taylor) Li; analysis and interpretation of results: Pengfei (Taylor) Li and Farzana Chowdhury; draft manuscript preparation: Farzana Chowdhury and Pengfei (Taylor) Li. All authors reviewed the results and approved the final version of the manuscript.

Declaration of Conflicting Interests

The author(s) declared no potential conflicts of interest with respect to the research, authorship, and/or publication of this article.

References

1. *Highway Capacity Manual 2010*. Transportation Research Board of the National Academies, Washington, D.C., 2010.
2. Abbas, M., D. Bullock, and A. Rhodes. Comparative Study of Theoretical, Simulation, and Field Platoon Data. *Traffic Engineering & Control*, Vol. 42, No. 7, 2001, pp. 232–236.
3. Abbas, M., D. Bullock, and L. Head. Real-Time Offset Transitioning Algorithm for Coordinating Traffic Signals. *Transportation Research Record: Journal of the Transportation Research Board*, 2001. 1748: 26–39.

4. Day, C. M., E. J. Smaglik, D. M. Bullock, and J. R. Sturdevant. Quantitative Evaluation of Fully Actuated versus Nonactuated Coordinated Phases. *Transportation Research Record: Journal of the Transportation Research Board*, 2008. 2080: 8–21.

5. Day, C. M., R. Haseman, H. Premachandra, T. M. Brennan, Jr, J. S. Wasson, J. R. Sturdevant, and D. M. Bullock. Evaluation of Arterial Signal Coordination: Methodologies for Visualizing High-Resolution Event Data and Measuring Travel Time. *Transportation Research Record: Journal of the Transportation Research Board*, 2010. 2192: 37–49.

6. Day, C. M., and D. M. Bullock. Computational Efficiency of Alternative Algorithms for Arterial Offset Optimization. *Transportation Research Record: Journal of the Transportation Research Board*, 2011. 2259: 37–47.

7. Day, C. M., H. Premachandra, T. M. Brennan, Jr, J. R. Sturdevant, and D. M. Bullock. Operational Evaluation of Wireless Magnetometer Vehicle Detectors at Signalized Intersection. *Transportation Research Record: Journal of the Transportation Research Board*, 2010. 2192: 11–23.

8. Liu, H. X., X. Wu, W. Ma, and H. Hu. Real-Time Queue Length Estimation for Congested Signalized Intersections. *Transportation Research Part C: Emerging Technologies*, Vol. 17, No. 4, 2009, pp. 412–427.

9. Wu, X., H. X. Liu, and D. Gettman. Identification of Oversaturated Intersections using High-Resolution Traffic Signal Data. *Transportation Research Part C: Emerging Technologies*, Vol. 18, No. 4, 2010, pp. 626–638.

10. Haseman, R. J., J. S. Wasson, and D. M. Bullock. Real-Time Measurement of Travel Time Delay in Work Zones and Evaluation Metrics using Bluetooth Probe Tracking. *Transportation Research Record: Journal of the Transportation Research Board*, 2010. 2169: 40–53.

11. Brennan, T. M. Jr, J. M. Ernst, C. M. Day, D. M. Bullock, J. V. Krogmeier, and M. Martchouk. Influence of Vertical Sensor Placement on Data Collection Efficiency from Bluetooth MAC Address Collection Devices. *Journal of Transportation Engineering*, Vol. 136, No. 12, 2010, pp. 1104–1109.

12. Day, C. M., S. M. Remias, H. Li, M. M. Mekker, M. L. McNamara, E. D. Cox, and D. M. Bullock. Performance Ranking of Arterial Corridors using Travel Time and Travel Time Reliability Metrics. *Transportation Research Record: Journal of the Transportation Research Board*, 2015. 2487: 44–54.

13. Hainen, A. M., J. S. Wasson, S. M. Hubbard, S. M. Remias, G. D. Farnsworth, and D. M. Bullock. Estimating Route Choice and Travel Time Reliability with Field Observations of Bluetooth Probe Vehicles. *Transportation Research Record: Journal of the Transportation Research Board*, 2011. 2256: 43–50.

14. Martchouk, M., F. Mannering, and D. Bullock. Analysis of Freeway Travel Time Variability using Bluetooth Detection. *Journal of Transportation Engineering*, Vol. 137, No. 10, 2010, pp. 697–704.

15. Young, S. E., E. Sharifi, C. M. Day, and D. M. Bullock. Visualizations of Travel Time Performance Based on Vehicle Reidentification Data. *Transportation Research Record: Journal of the Transportation Research Board*, 2017. 2646: 84–92.

16. Remias, S. M., A. M. Hainen, C. M. Day, T. M. Brennan, Jr, H. Li, E. Rivera-Hernandez, J. R. Sturdevant, S. E. Young, and D. M. Bullock. Performance Characterization of Arterial Traffic Flow with Probe Vehicle Data. *Transportation Research Record: Journal of the Transportation Research Board*, 2013. 2380: 10–21.

17. Tian, Z., V. Mangal, and H. Liu. Effectiveness of Lead–Lag Phasing on Progression Bandwidth. *Transportation Research Record: Journal of the Transportation Research Board*, 2008. 2080: 22–27.

18. Robertson, D. I. *Transit: A Traffic Network Study Tool*. Road Research Laboratory, Crowthorne, Berkshire, UK, 1969.

19. Day, C. M., and D. M. Bullock. Calibration of Platoon Dispersion Model with High-Resolution Signal Event Data. *Transportation Research Record: Journal of the Transportation Research Board*, 2012. 2311: 16–28.

20. Hainen, A. M., A. L. Stevens, R. S. Freije, C. M. Day, J. R. Sturdevant, and D. M. Bullock. High-Resolution Event-Based Data at Diamond Interchanges: Performance Measures and Optimization of Ring Displacement. *Transportation Research Record: Journal of the Transportation Research Board*, 2014. 2439: 12–26.

21. Newell, G. F. A Simplified Theory of Kinematic Waves in Highway Traffic, Part II: Queueing at Freeway Bottlenecks. *Transportation Research Part B: Methodological*, Vol. 27, No. 4, 1993, pp. 289–303.

22. Newell, G. F. A Simplified Theory of Kinematic Waves in Highway Traffic, Part I: General Theory. *Transportation Research Part B: Methodological*, Vol. 27, No. 4, 1993, pp. 281–287.

23. Kalman, R. E. A New Approach to Linear Filtering and Prediction Problems. *Journal of Basic Engineering*, Vol. 82, No. 1, 1960, pp. 35–45.

24. Roess, R. P., E. S. Prassas, and W. R. McShane. *Traffic Engineering*. Pearson/Prentice Hall, Hoboken, NJ, 2004.

25. Yin, Y., M. Li, and A. Skabardonis. Offline Offset Refiner for Coordinated Actuated Signal Control Systems. *Journal of Transportation Engineering*, Vol. 133, No. 7, 2007, pp. 423–432.